



Detection of Hypochromic Erythrocytes in Blood Smear by using Edge Contours of Cells as Trigonometric Projections

Muhammad Hamza Kamran¹, Zahra Rashid Khan², Javid Iqbal¹

¹School of Mechanical and Manufacturing Engineering (SMME), National University of Sciences and Technology (NUST), Islamabad, Pakistan

²NUST School of Health Sciences (NSHS), National University of Sciences and Technology (NUST), Islamabad, Pakistan

ARTICLE INFO

Keywords: Anemia, Overlap detection, Trigonometric projection, Peripheral blood smear

Correspondence to: Muhammad Hamza Kamran,
School of Mechanical and Manufacturing Engineering (SMME), National University of Sciences and Technology (NUST), Islamabad, Pakistan.
Email: mhkqureshi98@gmail.com

Declaration

Authors' Contribution

All authors equally contributed to the study and approved the final manuscript.

Conflict of Interest: No conflict of interest.

Funding: No funding received by the authors.

Article History

Received: 28-02-2026 Revised: 17-03-2026
Accepted: 26-03-2026 Published: 30-03-2026

ABSTRACT

Hypochromic microcytic anemia is a category of anemia in which the erythrocytes lacking hemoglobin content appear small with large central pallor. It is commonly caused by iron deficiency and thalassemia. The morphological analysis of hypochromic erythrocytes is done through peripheral blood smears (PBS) examination under a microscope. The manual procedure is a confirmatory step applied in analysis with complete blood count (CBC) and hematology analyzer. However, it is time-consuming and tedious. Blood smear analysis technique based on computer vision (CV) have been suggested to automate blood smear examination using digital images of microscopic view of blood film for various blood related disorder. One of the major challenges of CV is the detection of cells that overlap each other. The proposed method is a rule-based technique that utilizes trigonometric projection to segment overlapping cells and detect hypochromic erythrocyte by area of cell. The performance metric of the proposed method in detection of overlap in whole slide image (WSI) of iron deficiency blood is 97.40%, 78.94%, 87.10% for precision, recall and F1 score respectively. Regression analysis is also applied to demonstrates the importance of overlap segmentation in cell counting.

INTRODUCTION

Anemia is a condition indicating other underlying diseases Turner et al [2023](#). 41% of all pregnant women suffer from anemia Chaudhry and Kasarla [2023](#). It refers to lack of hemoglobin, low erythrocyte count and reduce hematocrit. Hypochromic microcytic anemia is a type of anemia in which the erythrocytes appear small in size (microcytic) with larger central pallor (hypochromic) Hee [1993](#). Iron deficiency anemia and thalassemia are the common cause of hypochromic microcytic anemia. Iron deficiency anemia is the most prevalent anemia type worldwide effecting 30.7% of women aged 15 to 49, 35.5% of pregnant women and 39.8% infants WHO [2025](#). Iron deficiency anemia occurs from low dietary iron intake, blood loss, increased iron requirement by the body such as in pregnant women and decreased nutrient absorption Warner Matthew J. [2023](#). Thalassemia is one of the common human genetic diseases highly prevalent in the Middle East, Mediterranean, Southeast and Central Asia Santo et al [2023](#). It is caused by reduction in alpha or

beta globin chain.

PBS examination is still relied upon for morphological analysis of blood cells. In PBS examination, drop of blood is smeared on the glass leaving three layers. Feather-edge layer is the thinnest layer containing mostly the platelets. The body is the thickest layer with blood cells too crowded to be observed. The monolayer is where the blood cells are investigated Buntin et al [2023](#). PBS examination acts as a confirmatory step in CBC analysis to minimize error Shams et al [2021](#). It is also integrated in automated hematology analyzer to improve accuracy. The analyzer if unable to detect entities leaves flags which are required to be examined under microscope N. et al [2025](#). Being an important procedure, PBS analysis is a time-consuming tedious task vulnerable to subjectivity Elmanina et al [2024](#).

Automation of PBS analysis is introduced to reduce the laborious task of manual analysis. This is achieved by computer aided diagnostics (CAD) that takes microscopic view as digital image, extract features and classify the

cells Shahzad et al [2024](#). WSI is a well-established digital image data in pathology education and research but limited in use for diagnosis Parwani [2021](#) due hindrance in applying in clinical setting and being an additional step of blood slide scanning. The application of WSI is difficult in cytopathology due to lack of depth in image Kumar et al [2020](#). However, researches have been carried to scan the whole blood smear for analysis of blood cells.

The CAD based analysis is an application of CV. The fundamental process of CAD and challenges of CV in automated blood cell analysis is segmentation and classification Baydargil and Bocklitz [2025](#). The techniques used for analysis are categorized as rule-based, machine learning (ML) and deep learning (DL). Rule-based techniques are widely used for their simplicity and efficiency, but they struggle in complex scenario Baydargil and Bocklitz [2025](#). ML brings great improvement to automated PBS analysis with demand of manually extracted features Margret [2025](#). DL surpasses ML as it automatically extracts feature for classification and segmentation. However, DL require large amount of high quality annotated images Margret [2025](#).

The proposed method is rule-based technique with aim to efficiently segment overlapping cells and classify hypochromic erythrocytes by area of cells from WSI of peripheral blood smear. The overlap segmentation technique is contour based in which on of the 2D coordinates of the contour of cells is projected on to angular domain for the detection of overlapping.

Motivation and Contribution

The goal of the research is to design rule-based methods for segmenting erythrocytes from low resolution WSI image using the contour of cells as 1D signal under low computation power while preserving the effectiveness of the performance of the method. Another motive is to determine the impact of overlap segmentation in automated cell counting.

The research introduces processing and analysis of objects in image as 1D signal by using single element of 2D coordinate of pixel as trigonometric projection to detect dip and segment overlapping. The research also contributes in segmentation of leukocytes and platelets by saturation value of Hue, Saturation and Value (HSV) image.

LITERATURE REVIEW

Purwar S. Purwar et al [2020](#) designed a ML based automated hypochromic microcytic anemia detection method in peripheral blood smear images. Multiple ML models were designed, tested and compared. The models were trained on features extracted from Convolutional Neural Network (CNN) and detect erythrocytes from those features. After performance measurements, the fused classifier of Neural Network, Support Vector Machine and K-Nearest Neighbor had the highest metrics compared to other ML achieving 99% in accuracy, 99% in specificity and 98% in sensitivity. The fused model is applied only on high resolution images for accurate classification. Arianti, N.D. Arianti et al [2023](#) trained mask Regional CNN (R-CNN) with 100 microscopic blood smear images to instantly segment and later classify the

erythrocytes in image. The model gained 80%, 69%, 60% and 60% in accuracy, precision, recall and F1 score at 60:40 data split, respectively.

Gil, T. proposed Taeyeon [2022](#) an automatic analysis method to detecting and classifying abnormal erythrocytes in blood smear images. To detect hypochromic erythrocytes, the cells are classified by the area of their central pallor. The image is segmented by Otsu threshold technique and the output is a binary image of white colored erythrocytes in black background. A simple threshold was then applied to obtain only the central pallor. The area was computed to classify hypochromic erythrocytes from the normal erythrocytes. The proposed method did not consider overlapped cells for classification of hypochromic cells.

Elsalamony, H.A. Elsalamony [2017](#) considered overlap segmentation before feature extraction of cell. To segment overlapping cells in an image, watershed transform is also used. Circle Hough Transform is applied to detect the cells by their roundness and bound the circular shape to the cell. Watershed transform is applied to separate the overlapping cells. After splitting, the radial signature is used as a feature to train neural network model and classify normal cells, sickle cells and elliptocytosis using the signature. No performance evaluation was done for the segmentation approach.

Naruenatthanaset, K. Naruenatthanaset et al [2021](#) developed a method to segment and classify erythrocytes from microscopic using deep learning models. To train the models, the images are first normalized and then the erythrocytes are segmented from the images. To segment the overlapping cells, concave point finding is applied to find the concave point which is the pixel of the inward bend where cells overlap. This point is used to fit ellipse contour shape for each cell in a cluster. The method achieved 88.81% in overlap separation.

An improvement is done by Miro-Nicolau M. Mir'o-Nicolau et al [2024](#) on the concave point finding for overlap segmentation. The part of contour that have high curvature are the interested regions. These regions are detected by a recursive procedure of comparing lengths and setting a threshold. Interest regions of cluster were selected, and concave points were computed. In the region, two points of a set distance are taken, and a midpoint is calculated. If a pixel coordinates of the concave point of contour is inside midpoint then the algorithm detects the point of overlapping. The model was tested applied to 16 microscopic blood smear images of ErythrocytesIDB2 dataset and compared with previous concave point finding methods. It achieved the highest in performance with results of 85.6% in precision, 86.1% recall and 85.8% in F1-score.

Dhar P. Dhar et al [2022](#) suggested a overlap segmentation technique by fast radial watershed system with seed point detection. For evaluation, the technique was applied to normal cells overlapping up to three cells achieving 98.81% precision, 98.6% recall and 98.7% in F1-score.

The state-of-the-art techniques for overlap segmentation discussed are tested on high resolution images. ML-based techniques have huge performance score, but require high resolution images and function at intense computation power. This limits them from clinical setting

of low resource. Recent rule-based techniques that are discussed are few that are properly tested. These are fast radial watershed system Dhar et al [2022](#) and improved concave point finding Mir'ó-Nicolau et al [2024](#). Fast radial watershed system was thoroughly tested with multiple datasets, but for normal erythrocytes overlapping upto three cells maximum. The improved concave point finding was tested on blood smear images of sickle cell anemia only.

METHODOLOGY

The proposed method is designed and applied for WSI of blood smear by J. Guilherme de Almeida Almeida [2023](#). The library of OpenCV is used to process the image and trace contour of cells Bradski [2000](#). ScipPy is used for peak detection of the trigonometric projection Virtanen et al [2020](#) and matplotlib is used to visualize the graphs for 2D contour and 1D projection Virtanen et al [2020](#).

Image acquisition

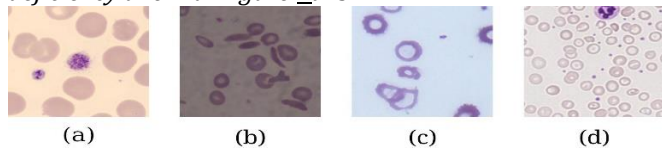
The microscopic image of blood smear slide labeled as IX 2 is obtained as BigTiff format Almeida [2023](#). This file format is most common in histology image acquisition. Sections of monolayer are cropped out from the file using the Bio-Format tool Besson et al [2019](#). The overlapping cells are marked and counted by professional in hematology as ground truth for performance evaluation of the method in overlap segmentation.

To further test the overlap segmentation, different datasets are also acquired. These include digital microscope view of blood smear by K. Naruenatthanaset Naruenatthanaset et al [2021](#) labeled Iron deficiency anemia, images of normal erythrocytes captured by CellaVision DM96 labeled as PBC dataset normal DIB Acevedo et al [2020](#) and mask image of sickle cell anemia blood smear image labeled erythrocytesIDB2 Gonzalez-Hidalgo et al [n.d.](#)

The segmentation procedures discussed only applies to IX 2 since the regression based analysis of the proposed method is only applied on this dataset.

Figure 1

Preview of the datasets. Figure [1a](#) is PBC dataset normal DIB. Figure [1b](#) is erythrocytesIDB2. Figure [1c](#) is Iron deficiency anemia. Figure [1d](#) is IX 2.



Segmentation of leukocyte and platelets

For detection and classification of erythrocytes, unwanted entities in the image must be excluded. In the peripheral blood smear image, these entities are leukocytes and platelets which have a more saturated color than erythrocytes. The color space of image is converted from red, blue, green (RGB) into hue, saturation, value (HSV). HSV color space is best suited for segmenting the image Masoudi [2022](#). HSV color space image is best suited color feature for machine learning algorithm in cell classification and leukemia detection Dese et al [2021](#). Saturation of the HSV color space that defines the brightness of image provided better result in

color detection. Mean saturation value is taken from the leukocytes and platelets and used to set the threshold to replace all leukocytes and platelets with white pixel.

Algorithm 1 Segment leukocyte and platelets

Require: Copy of input image as HSV

Ensure: RGB image with leukocytes and platelets whiten out

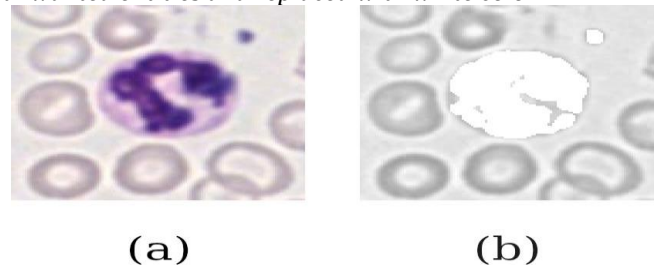
1: **if** Saturation > 45 **then**

2: RGB ← 255, 255, 255

3: **end if**

Figure 2

Figure [2a](#) shows blood smear image with leukocyte and platelets. Figure [2b](#) shows the segmentation of the unwanted entities and replaced with white color



Segmentation of Erythrocyte

The color image is then converted into a gray-scale image and smoothed by Gaussian blurring. For segmentation of RBC, the gray-scale is converted into a binary image by Otsu method. Otsu method separates background and foreground by difference in variation of light intensity Al-Rahlawee and Rahebi [2021](#). The erythrocytes appear as white and background as black. The hypochromic cells have large holes and normal cells have small or no holes. Distance transform is applied to exaggerate the bend at overlapping site of clustered cells.

Algorithm 2 Segment erythrocytes

Require: RGB image of erythrocytes

Ensure: Binary image of white cells in black background

1: Convert RGB image to grayscale image

2: Apply Otsu threshold

3: invert black and white image

Figure 3

Figure [3a](#) shows the greyscale of two overlapping RBCs. Figure [3b](#) shows the segmentation of RBC from background as binary image



Edge tracing

Edges of the white colored objects in black background in binary image is detected by the change in color. The coordinates at which the color of pixel changes, its pixel is stored as 2D discrete array. The hierarchy system is also generated where the outer contour is the parent and the inner contour is the child. This system is used to keep the data organized for later total area calculation for classification of erythrocytes. The edge tracing technique

applied is referred as border following algorithm by Suzuki S. Satoshi Suzuki [1985](#).

Algorithm 3 Trace erythrocyte

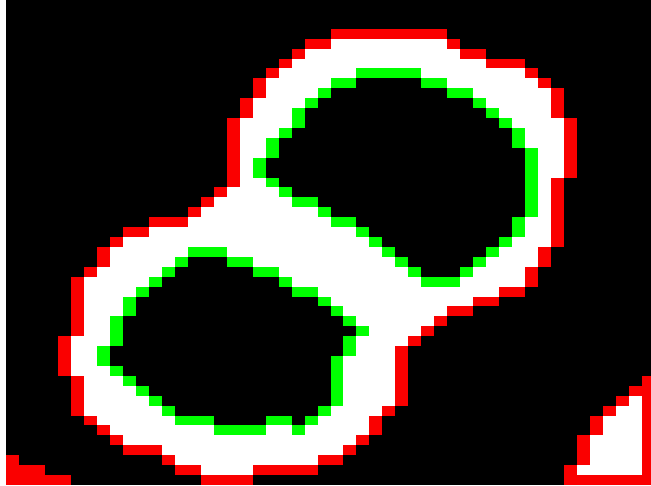
Require: Binary image of erythrocytes

Ensure: 2D array of contour of cells

- 1: Apply distance transform to binary image
- 2: Trace contour of image

Figure 4

Binary image of RBCs with outer contour highlighted in red color and inner contour highlighted in green color



Contour Transformation

The pixel coordinates of the contour is translated so that the centroid is at the origin. The major axis of the contour is determined to compute for angle. This angle is applied to rotation matrix to rotate the contour shape so that its major axis is horizontally flat.

$$\theta = \arctan(\text{major axis}) \quad (1)$$

$$x = [\cos\theta \quad \sin\theta] \quad (2)$$

$$y = [-\sin\theta \quad \cos\theta]$$

Algorithm 4 Translate and rotate contour

Require: Outer contour of cells

Ensure: Contour position with centroid at origin and major axis horizontal

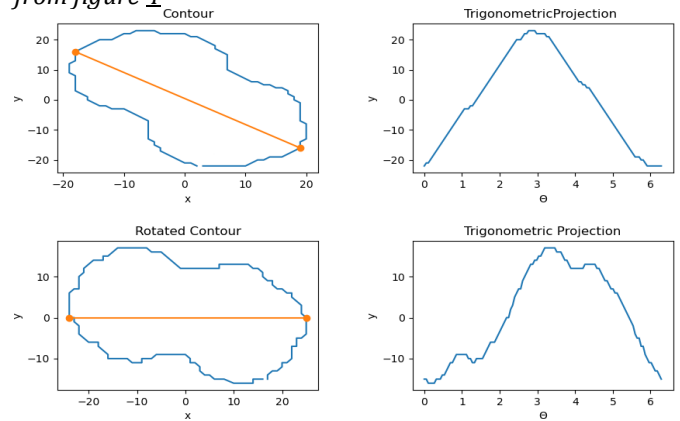
- 1: Compute moments of contour
- 2: Compute centroid coordinate of contour
- 3: Subtract contour coordinates by centroid coordinates
- 4: Calculate radii
- 5: Get 2D coordinate of contour for the longest radius
- 6: Calculate distance of the 2D Coordinate with other coordinates of contour
- 7: Get 2D coordinates of the longest distance (major axis)
- 8: Calculate slope of the major axis
- 9: Compute angle using arctan function
- 10: Apply negative value of angle to rotation matrix

Trigonometric Projection

With major axis being horizontally flat, the y-coordinates of the contour is projected in angular domain. Trigonometric projection varies with rotation which can hide away the peaks necessary for overlap segmentation. So criteria is set in which the x-coordinate of major axis of shape is 0 to obtain the desired signal as shown in figure.

Figure 5

Trigonometric projection of contour of overlapping cells from figure 4



The signal is then smoothened by moving average and split into two parts at π leaving a maxima extrema and minima extrema.

Algorithm 5 Trigonometric projection of contour

Require: 2D transformed contour

Ensure: trigonometric projection sub-divided into two

- 1: Get y-coordinate as a separate array from contour
- 2: Apply moving average filter to the trigonometric projection
- 3: Create array (l) of equally spaced value from 0 to 2π of length equal to that of the signal
- 4: **if** $3.2 < \text{element}_i < 3.1$ **then**
- 5: u= position of element
- 6: **end if**
- 7: signal1= first value to u^{th} value of trigonometric projection
- 8: signal2= u^{th} value to last value of trigonometric projection

Peak Detection

Maxima extrema is directly analyzed. The peaks of minima extrema appear as dips. So it is flipped by applying absolute to all the values in the minima extrema. The consecutive values of each are differentiated throughout the 1D array. This difference is called slope. Towards the peak, the slope is positive, and it is negative after the peak. The shift in polarity of the slope allows the computer to detect the peak. Once the peak is detected for each signal, comparison among them is done. The half signal with the most peak is selected. The peaks are then used to find the middle point that will be used to later segment cell cluster.

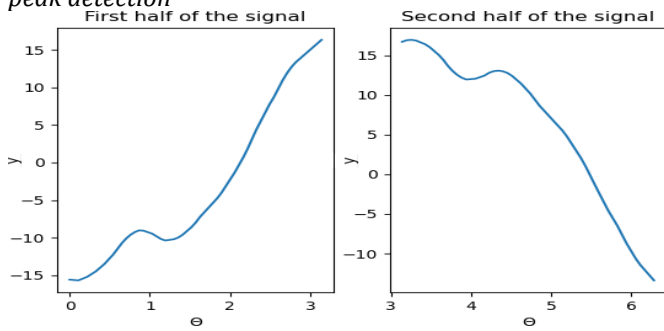
Algorithm 6 Detection of peak

Require: 1D signal

Ensure: number of peaks

- 1: **if** signal is minima extrema **then**
- 2: signal = -signal
- 3: **end if**
- 4: find peaks in signal

Figure 6
Trigonometric projection filtered and split at half cycle for peak detection



Overlap Segmentation

Midpoint between two consecutive peak points is calculated by taking their average. This value obtained from trigonometric tracing describes which 2D coordinate is detected as a concave of the contour. This coordinate is taken as the initial point from which the line will begin to be drawn. To accurately split the shape into two near halves, a vertical line is best suited. The end point of the line will be the at the same x-coordinate value with y-coordinate at the opposite side of the contour. With last coordinate set, a black line of two pixel width is drawn to split the cells into two. The segmented binary image is traced again with new contour where the overlapping cells are split.

Algorithm 7 Splitting cells

- Require:** Binary image, coordinates of peak
- Ensure:** Binary image with overlapped cells split
- 1: Calculate distance between two peak
- 2: Calculate start point by computing middle position of distance
- 3: x-coordinate of end point = x-coordinate of start point
- 4: **if** y-coordinate of start point < 0 **then**
- 5: y-coordinate of end point = 20 - y-coordinate of start point
- 6: **end if**
- 7: **if** y-coordinate of start point > 0 **then**
- 8: y-coordinate of end point = 20 + y-coordinate of start point
- 9: **end if**
- 10: Transform the points to original position of contour
- 11: Draw black line from start point to end point

Figure 7
In figure 7 blue circles represents peak and orange triangle represents the midpoint

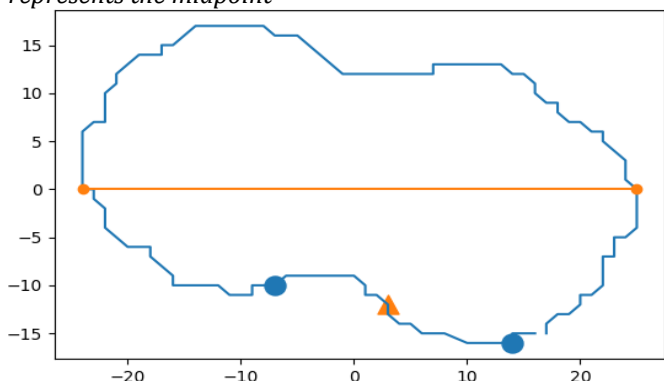
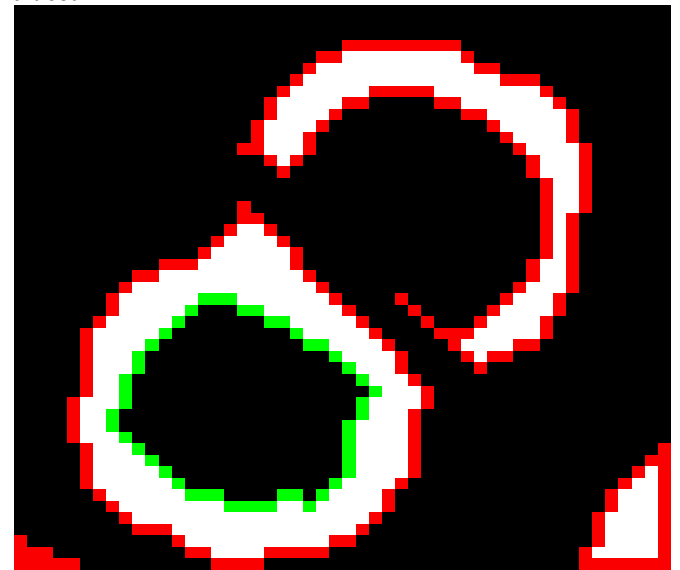


Figure 8
Overlapping RBCs split into two and their contour re-traced



Computation of Area and Circularity

Hypochromic cells and normal cells are classified by the area of the cell contour is calculated. Area of the outer contour is compared with its inner contour. The larger the pallor of cell, the larger the area of the inner contour. In total, the normal cell will have larger total area compared to the area of hypochromic cells. The area of the contour is calculated by using shoelace formula. This formula is widely used to calculate area of a enclosed and non-intersected polygon by splitting the polygon into trapezoidal strips Dumka and Mishra 2025.

$$Area = \sum |(x_i * y_{i+1}) - (x_{i+1} * y_i)| \quad (3)$$

In case of certain severe hypochromic cells, the segmentation forms a gap in the tori shaped cell resulting in the contour to appear crescent shaped. The contour of the shape when converted to 1D signal results in a dip. With this dip, the algorithm will count one cell as two cells. To overcome this error, circularity of 2D contour is used to detect crescent shape and round shape objects. Circularity is parameter, that describes the roundness of shape. When the crescent shape is detected, the algorithm will divide the dip counts by two.

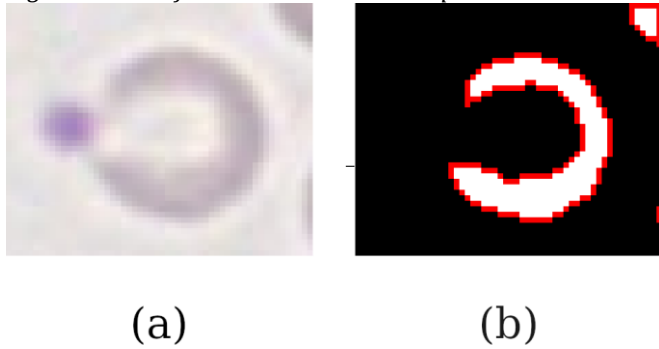
$$Circularity = \frac{4 * \pi * Area}{Perimeter} \quad (4)$$

Experiment Design

The performance of the proposed method in overlap segmentation is evaluated on precision, recall and F1-score. These three parameters are best suited for defining the effectiveness of the method. Accuracy is not considered as it only defines the overall performance of the method in all classification and can't be used in dataset where there is an imbalance of true positive and true negative Obi 2023. True positive (TP) is the actual cell detected. False positive (FP) is the cell detected that doesnot exist. False negative (FN) is cell undetected. True negative is

Figure 9
Figure 9a shows hypochromic RBC. Figure 9b shows the

segmentation of the cell as crescent shaped



Algorithm 8 Classification of cells by area
Require: contours of cells from overlap segmented image
Ensure: Number of cells
 1: total cells = 0
 2: hypochromic cells = 0
 3: Calculate area of contours by shoelace theorem
 4: Total Area = Outer contour - Inner contour
 5: **if** Total Area > 450 **then**
 6: total cells += 1
 7: **end if**
 8: **if** 200 > Area < 450 **then**
 9: hypochromic cells += 1
 10: **end if**

The signal data that is not a dip and is disregarded in image object detection as it will make the performance of method appear higher.

The performance is done to overlapping cells only from the datasets. The proposed method is tested on 40 cell clusters from IX 2, 64 from Iron deficiency anemia, 30 from PBC dataset normal DIB and 102 from erythrocytesIDB2. Due to large pixel density the images of the dataset except IX 2 are downsized by half, so the method can perform effectively.

To test the method in cell counting, regression based analysis is applied. The method is evaluated on root-mean-square error (RMSE), mean absolute error (MAE) and coefficient of determination (R^2). The actual value is determined by manually counting the cells in the image multiple times. The most occurring count is taken as actual value.

RESULT AND DISCUSSION

For IX 2 dataset, the proposed method detected erythrocytes in the digital image by labeling them within a box as demonstrated in figure.

Figure 10

The rectangles generated by the algorithm represents the cell detected by the proposed method

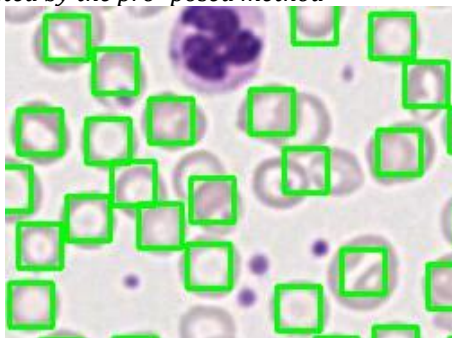


Table below describes the performance of the method in multiple dataset. The proposed method achieved similar F1 score for diverse images. This is possible by addition of extra step of resizing all the dataset except IX 2 by half of the original size. The proposed method achieved high precision at IX 2 and high recall at PBC dataset normal DIB.

Table 1

Performance Evaluation of Proposed Method in Overlap Segmentation

S.No.	Sample	Precision	Recall	F1-Score
1	IX 2	97.40%	78.94%	87.10%
2	Iron deficiency anemia	95.03%	77.45%	85.35%
3	PBC dataset normal DIB	88.40%	85.91%	87.14%
4	erythrocytesIDB2	97.23%	77.19%	86.06%

The proposed method is compared with state-of-art concave point finding by Miro-Nicolau

M. Mir’o-Nicolau et al 2024 which was tested on erythrocytesIDB2 dataset in 3. The proposed method gained highest precision but low recall in result. By overall performance, both method have similar F1-score. Low recall of the proposed method is due to the presence of elongated cells and sickle cells in overlapping cluster.

Two randomly selected sections of the peripheral blood smear image, IX_1 were selected for regression analysis. Figure 12 and figure 13 shows the number of erythrocytes detected by the method with overlap segmented image and without overlap segmented image of the dataset. Without overlap segmented, the method counts the cluster of erythrocytes as a single cell. The difference in dataset "1" is noticeable than compared to dataset "2".

Evaluation in regression analysis is applied using RMSE, MAE and R^2 . Low RMSE and MAE indicates that the automated count by the method is more accurate and closer to actual

Table 2

Performance Comparison in Detecting Overlapping Cells

S.No.	Method	Precision	Recall	F1-score
1	Proposed Method	97.23%	77.19%	86.06%
2	Miro-Nicolau M. Mir’o-Nicolau et al 2024	85.6%	86.1%	85.8%

Table 3

Performance Comparison in Detecting Overlapping Cells

S.No.	Method	Actual count	Predicted	Accuracy
1	Proposed Method	173	141	81.7%
2	Miro-Nicolau M. Mir’o-Nicolau et al 2024	277	246	88.9%

Figure 11
Radar Chart of Result Comparison

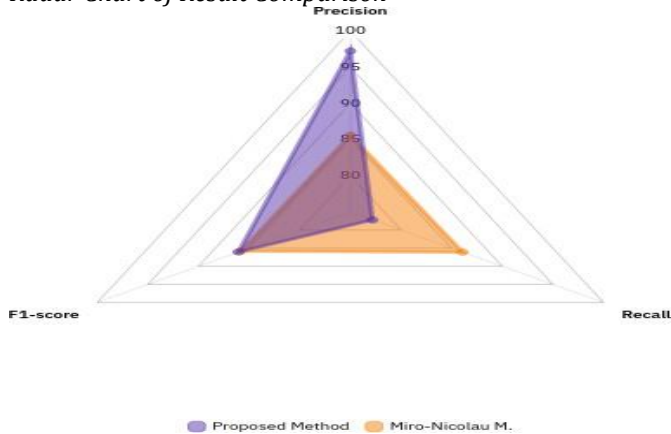


Figure 12
Total Erythrocyte Count
Total erythrocyte counting

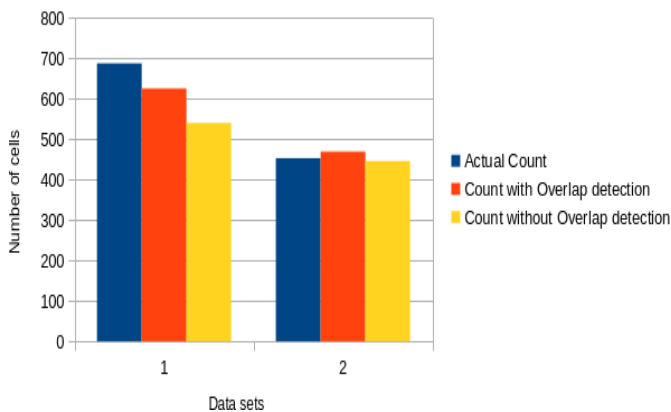
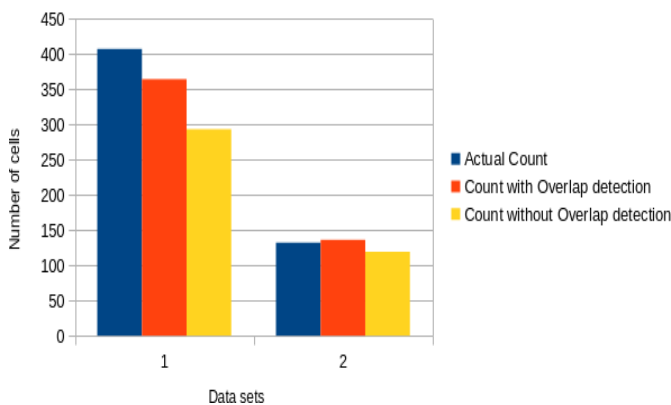


Figure 13
Hypochromic Erythrocyte Count
Hypochromic erythrocyte counting



REFERENCES

- Acevedo, Andrea et al. 2020. A dataset for microscopic peripheral blood cell images for development of automatic recognition systems. <https://doi.org/10.1016/j.dib.2020.105474>
- Almeida, Jos'e Guilherme de. 2023. Peripheral blood smears from individuals with mds or anaemia, and controls. BioStudies,S-BIAD440 <https://doi.org/www.ebi.ac.uk/biostudies/bioimages/studies/S-BIAD440>.
- Arianti, Nunik Destria, Ahmad, Norashikin and Muda,

value. High R^2 shows that the method is best fit. With segmentation of overlapping, the method achieved much higher result compared with itself without overlap segmentation, gaining 45.27 in RMSE, 39.00 in MAE and 0.88 in R^2 .

Table 4
Regression Analysis of Total Erythrocyte Count

S.No.	Condition	RMSE	MAE	R^2
1	with overlap segmentation	45.27	39.00	0.88
2	without overlap segmentation	104.06	77.00	0.37

Table 5
Regression Analysis of Hypochromic Erythrocyte Count

S.No.	condition	RMSE	MAE	R^2
1	with overlap segmentation	30.54	23.5	0.95
2	without overlap segmentation	76.91	63.5	0.65

CONCLUSION

Overlap detection using trigonometric projection is an effective and efficient approach for overlap segmentation for accurate enumeration of erythrocyte in PBS image. The overlap detection of cell clusters by the edges as 1D signal reduces memory usage and computation power allowing automated analysis of large image size of blood smear scan.

The method proposed is a rule-based technique applied for the WSI dataset of captured by Hamamatsu Nanozoomer with parameter specified for segmentation of red blood cells from the image and classification. The method poses as a strong candidate for low resolution images. The overlap segmentation technique is hindered by high resolution of object in image. This can be overcome by reducing the size of image.

The implemented code and overlapped images of IX 2 used to test the method is provided to allow researchers to determine metrics and conduct research in the given overlapped images

(<https://github.com/HK2598/Hypochromic-erythrocyte-detection-by-cell-edges-as-trigonometric-projection>).

Ethical Approval: No human participants or animal were involved for the study.

Contribution: Conceptualization: M.H. Kamran; Methodology: M.H. Kamran; Data curation: M.H. Kamran, Z.R. Khan; Writing-review and editing: M.H. Kamran, J. Iqbal

Data availability: The data and source code of the study are available in GitHub repository.

<https://github.com/HK2598/Hypochromic-erythrocyte-detection-by-cell-edges-as-trigonometric-projection>.

Azah Kamilak. 2023. Classification of overlapping red blood cells using image segmentation and convolutional neural network. Internation Journal of Computer Information Systems and Industrial Management Applications. 15.

4. Baydargil, Husnu Baris and Bocklitz, Thomas. 2025. Unstained blood smear analysis: a review of rule- based, machine learning and deep learning technique. Journal of Biophotonics. 18(10). <https://doi.org/10.1002/jbio.202500121>

5. Besson, S. et al. 2019. Bringing open data to whole slide

- imaging. Digital Pathology. 11435: pp. 3–10
<https://doi.org/10.1007/978-3-030-23937-4.1>.
6. Bradski, Gary. 2000. The opencv library. Dr. Dobb's Journal of Software Tools. 120: pp. 122–125. Buntin, S. T., Liang, X., Paessler, M. E. and Chonat, S. 2023. Peripheral blood smear review. Atlas of Pediatric Hematopathology. Pp. 1–8
 7. Chaudhry, Hammad S. and Kasarla, Madhukar Reddy. 2023. Microcytic hypochromic anemia. StatPearls Publishing.
 8. Dese, Kokeb et al. 2021. Accurate machine-learning-based classification of leukemia from blood smear images. Clinial Lymphoma, Myeloma and Leukemia. 21(11): e903–e914.
<https://doi.org/10.1016/j.clml.2021.06.025>
 9. Dhar, Prasenjit, Devi, K. Suganya, Satti, Satish Kumar and Srinivasan, P. 2022. Efficient detection and partitioning of overlapped red blood cells using image processing approach. Innovation System Software Engineering. 21: pp. 79–91
<https://doi.org/10.1007/s11334-022-00478-y>.
 10. Dumka, Pankaj and Mishra, Dhananiay R. 2025. The shoelace algorithm in engineering: python applications for area and internal analysis. Barekeng: Journal of Mathematics and Its Applications. 19(3): pp. 1673–1648
<https://doi.org/10.30598/barekengvol19iss3pp1637-1648>.
 11. Elmann, Mohammad, Elsafty, Ahmed, Ahmed, Yomna, Rushdi, Muhammad and Morsy, Ahmed. 2024. Deep learning segmentaion and classification of red blood cells using a large multi-scanner dataset. arXiv preprint.
 12. Elsalamony, Hany A. 2017. Anaemia cells detection based on shape signature using neural networks. Measurement. 104: pp. 50–59.
<https://doi.org/10.1016/j.measurement.2017.03.012>
 13. Gonzalez-Hidalgo, M., Guerrero-Pena, F., Herold-Garcia, S., Jaume-i-Capo, A. and Marrero-Fernandez, P.D. Red blood cell cluster separation from digital images for use in sickle cell disease. Hee, Shan Que. 1993. Biological monitoring: an introduction. Wiley.
<https://doi.org/10.1109/jbhi.2014.2356402>
 14. Kumar, Neeta, Gupta, Ruchika and Gupta, Sanjuy. 2020. Whole slide imaging (wsi) in pathology: current perspectives and future direction. Journal of Digital Imaging. 33(4): pp. 1034–1040.
<https://doi.org/10.1007/s10278-020-00351-z>
 15. Margret, Isaac Neha. 2025. Deep learning techniques for analyzing peripheral blood smears: a meta analysis. Neural Computing and Application. 37: pp. 18039–18065.
<https://doi.org/10.1007/s00521-025-11401-4>
 16. Masoudi, Babak. 2022. Vks:a pre-trained deep network with attention mechanism to diagnose acute lymphoblastic leukemia. Multimedia Tools and Applications. 82: pp. 18967–18983.
<https://doi.org/10.1007/s11042-022-14212-0>
 17. Miró-Nicolau, Miquel, Moyà-Alcover, Gabriel and González-Hidalgo, manuel. 2024. Improving concave point detection to better segment overlapped objects in images. Multimed Tools Appl. 83: pp. 24339–24359.
<https://doi.org/10.1007/s11042-023-15382-1>
 18. N., Fareed, Y., Jamal Siddiqi M., S., Aman and G., Fatima. 2025. Comparison of automated hematology analyzer (xn 1000) flags and peripheral blood smear examination: an experience from a tertiary care hospital. Indus Journal of Bioscience Research. 3(6): pp. 445–448
<https://dx.doi.org/10.70749/ijbr.v3i6.1413>.
 19. Naruenatthanaset, Korranat, Chalidabhongse, Thanarat H., Palasuwan, Duangdao, Anantrasirichai, Nan- theera and Palasuwan, Attakorn. 2021. Red blood cell segmentation with overlapping cell separation and classification on imbalanced dataset.
 20. Obi, Jude Chukwura. 2023. A comparative study of several classification metrics and their performances on data. World Journal of Advanced Engineering Technology and Sciences. 8(1): pp. 308–314
<https://doi.org/10.30574/wjaets.2023.8.1.0054>.
 21. Parwani, Anil V. 2021. Whole slide imaging: current application and future directions. Springer international publishing.
https://doi.org/10.1007/978-3-030-83332-9_3
 22. Purwar, Shikha, Tripathi, Rajiv Kumar, Ranjan, Ravi and Saxena, Renu. 2020. Detection of microcytic hypochromia using cbc and blood film features extracted from convolution neural network by different classifiers. Multimed Tools Appl. 79(8): pp. 4573–4595
<https://doi.org/10.1007/s11042-019-07927-0>.
 23. Al-Rahlawee, Anfal Thaer hussein and Rahebi, Havad. 2021. Multilevel thresholding of images with improved otsu thresholding by black widow optimization algorithm. Multimed Tools Appl. 80: p. 28217
<https://doi.org/10.1007/s11042-021-10860-w>.
 24. Santo, Daniela et al. 2023. Prevalance rate of thalassemia carriers among individual with microcytosis or hypochromia in portugal. Acta Medica. 36(7-8): pp. 467–474
<https://doi.org/10.20344/amp.19162>.
 25. Satoshi Suzuki, KeiichiA be. 1985. Topological structural analysis of digitized binary images by border following. Computer Vision, Graphics and Image Processing. 30(1): pp. 32–46
[https://doi.org/10.1016/0734-189X\(85\)90016-7](https://doi.org/10.1016/0734-189X(85)90016-7).
 26. Shahzad, Muhammad et al. 2024. Blood cell image segmentation and classification: a systematic review. Peer J Comput Sci. 10: e1813.
<https://doi.org/10.7717/peerj-cs.1813>.
 27. Shams, Usman Ali et al. 2021. Bio-net dataset: ai-based diagnostic solutions using peripheral blood smearimages. Blood Cells, Molecules and Disease. 105: p. 102823
<https://doi.org/10.1016/j.bcmd.2024.102823>.
 28. Taeyeon, Gil. 2022. Automatic analysis system for abnormal red blood cells in peripheral blood smear. Microsc Res Tech. 85(11): pp. 3623–3632
<https://doi.org/10.1002/jemt.24215>.
 29. Turner, Jake, Parsi, Meghana and Badireddy, Madhu. 2023. Anemia. StatPearls Publishing. www.ncbi.nlm.nih.gov/books/ Virtanen, Pauli, Gommers, Ralf and Oliphant, Travis E. 2020. Scipy 1.0: fundamental algorithms for scientific computing in python. Nature Methods. 17: pp. 261–272
 30. Warner Matthew J., Muhammad T. Kamran. 2023. Iron deficiency anemia. StatPearls Publishing. WHO. 2025. Who global anaemia estimates: key findings. World Health Organization.